**NTNU**

Norwegian University of
Science and Technology

# AEP based on rotor equivalent wind speed measured from a floating LiDAR

**Eduardo Tormo Soler**

# AEP based on rotor equivalent wind speed measured from a floating LIDAR

Eduardo Tormo Soler

Department of Energy and Process Engineering, Norwegian University of Science and Technology, Trondheim, Norway

**Abstract.** During the last years, the wind turbines rotor area and the hub height have been increasing gradually. This has entailed new challenges for the measuring atmospheric boundary layer techniques which must be able to measure wind speeds over 200m height and also the use of the hub height wind speed for estimating the rotor power has been questioned. In this study, three boundary layer estimation methods have been compared with wind data from a floating LIDAR buoy, in order to analyze their behaviour and their reliability. Subsequently, the REWS theory for the energy estimation has been tested against the hub height wind speed in order to determine the power production difference. From the three boundary layer estimation methods studied, the logarithm law and the power law get excellent results when they were compared to long term average LIDAR measurements are estimated, obtaining MSE of 0.0031 and 0.0087 respectively. However the results from 10-minute average boundary layer were very inaccurate with maximum MSE of 19. On the other hand, the energy estimation results show that the use of hub height wind speed overestimates the wind turbine power production around 0.2% for LL and PL and, 0.4% when LIDAR measurements are used. Thus, it can be concluded that REWS method implementation does not imply big changes on AEP.

## Abbreviations

| | | | |
|---|---|---|---|
| ABL | Atmospheric Boundary Layer | MOST | Monin-Obukhov Similarity Theory |
| AEP | Annual Estimation Power | | |
| HH | Hub Height | MSE | Mean Square Error |
| HKZ | Hollandse Kust Zuid | NREL | National Renewable Energy Laboratory |
| LIDAR | (Light Detection And Ranging | | |
| | | PL | Power Law |
| LL | Logarithm Law | REWS | Rotor Equivalent Wind speed |
| MBL | Mean Boundary Layer | STD | Power Law using $\alpha = 0.14$ |

## 1. Introduction

In recent decades, the wind power production has suffered a huge development in practically every part of the world, increasing the installed power from 10 to 40% per year [4]. This development is based on the wind turbines size increment and the offshore areas utilization for installing wind turbines. In fact, the European Union 2012 roadmap for renewable energy sources establish the northern sea as most promising european area for wind power production [15]. In order to achieve this goal, new technology improvements

are required in order to install wind turbines in deeper waters [4].

Regarding to the wind turbines increasing size, in the last 30 years the rotor diameter has increased from 30 to 160m and the wind turbine production from 0.5-10MW [13]. The wind turbines size increment has entailed a new challenge for the wind currents study and the annual energy estimation. For the power calculation, the wind speed at hub height has been used for that purpose however, with rotor diameters constantly increasing, the hub height velocity could not be representative of the wind distribution over the rotor. The REWS method is believed to estimate a most representative wind speed over the rotor.

The second challenge is to improve the atmospheric boundary layer measurements when those big-sized wind turbines are installed. For years, the wind currents have been measured by using anemometers placed in along met masts. Nowadays, since wind measurements at higher heights are required, the use of met masts have been restricted due to their implementation cost increases with the cube of the met mast height [16]. One alternative is using met masts for measuring wind speeds at low heights and next, use atmospheric boundary layer estimation methods such as Logarithm law , Power Law [8] or MOST [9]. An innovative alternative is LIDAR technology. Its entry for the wind measurement has supposed a new revolution on the business especially for the offshore wind farms development. The measurement range, the accuracy and the ability for measuring winds at different heights make of that technique, one of the most projected methods for wind measurements for the next years [16]. Though, this technology presents some disadvantages, specially the buoy motion influence on the measurements for floating LIDAR devices.

Along this document, these LIDAR limitations will be detailed and LIDAR measurements, from a floating buoy located in the dutch section of the north sea, will be compared with several ABL estimation methods in order to study their performance. Several AEP estimations will be calculated by combining some parameters such as the LIDAR and the three ABL estimation methods, named above; considering the the hub height wind speed and the REWS; and using power curves from DTU 10-MW and NREL 5-MW wind turbines.

## 2. Methodology

*2.1. logarithm Law*

The logarithm Law (LL), Eq. (1), is a common used boundary layer prediction method. The method is based on the MOST method [9], represented in the Eq. (2).

$$u_2 = u_1 \frac{ln(z_2/z_0)}{ln(z_1/z_0)} \tag{1}$$

$$u_2 = u_1 \frac{ln(\frac{z_2}{z_0}) - \psi(\frac{z_2}{L_0}))}{ln(\frac{z_1}{z_0}) - \psi(\frac{z_2}{L_0})} \tag{2}$$

Where:

| | |
|---|---|
| $u_1$ | is the wind speed at reference height, 40m |
| $u_2$ | is the estimated wind speed |
| $z_0$ | is the roughness length |
| $z_1$ | is the reference height, 40m |
| $z_2$ | is the height where the wind speed is estimated |
| $\psi$ | is the atmospheric stability parameter |
| $L_0$ | is the Obuckhov Length |

The LL application does not consider the atmospheric stability and assume neutral atmospheric conditions ($\psi = 0$). The MOST method bases its accuracy in include the atmospheric stability and the heat exchange influence on the boundary layer. Nevertheless, as explained by Fechner [9], MOST method is only valid under stationary conditions and within surface layer height >70. When the mentioned conditions were applied to the HKZ data, the number of time points that met these specifications were less than 50%. Thus, the obtained results could not be extrapolated for the Annual energy estimation.

The standard value of $z_0$ under open sea with waves conditions could be assumed between $[0.0001 - 0.01]$ [14]. In this study the roughness length has been set to 0.001m.

### 2.2. Power Law

The power law method (PL) is an other ABL estimating methods that considers the relation of the increasing wind speed with the height could be approached with an exponential function, as shown in Eq. (3). Therefore, for estimating the wind shear exponent, are only required wind speed measurements at two heights. The wind speeds at 40 and 120m have been used for the coefficient calculation at each time point. Afterwards, the estimated boundary layer has been calculated with this coefficient and the wind speed at 40m.

$$u_2 = u_1 \left( \frac{z_2}{z_1} \right)^\alpha \tag{3}$$

Where:
$u_1$        is the wind speed at reference height, 40m
$u_2$        is the estimated wind speed
$z_1$        is the reference height, 40m
$z_2$        is the height where the wind speed is estimated
$\alpha$        is the wind shear coefficient

That method has been deeply studied and it has been established some standard wind shear coefficients for different locations. On IEC 61400-3, the wind shear coefficient at open sea locations is set to 0.14 (STD). This standard coefficient value has been also analysed for testing its reliability, using the Eq.(3) and the wind speeds at 40m.

### 2.3. Rotor Equivalent Wind Speed

Over the years, the wind turbines power production has been increased by rotor size increment. Since the production depends on the horizontal wind speed distribution over the rotor, with the latest size increment it looks less accurate to assume the hub height wind speed as a representative wind speed over the turbine. The REWS method purpose is to estimate the kinetic flux through the rotor area by weighting wind speeds from different heights inside the rotor [11]. The weighting procedure consists in dividing the rotor area in several horizontal segments. It is considered a constant wind speed for each segment thus, wind speed measurements at several heights are required. The weight for each velocity will be the relation between the segment area, which the wind velocity is assigned, and the total rotor area.

According to IEC 61400-12-1 [5], the rotor equivalent wind speed has to be calculated with the Eq. (4).

$$V_{eq} = \left( \sum_{i=1}^{n_h} u_i^3 \frac{A_i}{A} \right)^{1/3} \tag{4}$$

Where:

| | |
|---|---|
| $n_h$ | is the number of available measurement heights |
| $u_i$ | is the 10 min average wind speed measured at height $i$ |
| $A$ | is the complete area swept by the rotor |
| $A_i$ | is the area of the $i$ th segment, i.e. the segment the wind speed $u_i$ is representative |

For the wind turbine power estimation, the $u_i$ component perpendicular to rotor area must be considered. That requirement is included on Eq.(5) [6]. In this equation the upflow angle and the wind shear are considered. To facilitate the study, is assumed that the wind turbine is rotating instantaneously, producing energy of wind speeds from all directions. It has been assumed that the wind direction at hub height is always perpendicular to rotor area therefore, for the rest of heights, the wind speed component for the assumed main direction has been calculated.

$$REWS = \sqrt[3]{\frac{1}{A} \sum_{i=1}^{n_h} \left( u_x(h_i) \cdot \cos(\beta(h_i)) \cdot \frac{\cos(\beta(h_i))}{\cos(\theta(h_i) + \theta_{tilt})} \right)^3 \cdot A_i} \tag{5}$$

Where:

| | |
|---|---|
| $u_x(h_i)$ | is the horizontal wind speed at height $i$ |
| $\beta(h_i)$ | is the wind direction at height $i$ relative to wind direction at hub height |
| $\theta(h_i)$ | is the upflow angle at height $i$ |
| $\theta_{tilt}$ | is the wind turbine rotor tilt angle with respect to the vertical |

For the study, the tilt angle is assumed $\theta_{tilt} = 0$.

The segments with areas $A_i$ must to be set considering that the point, where the wind speed is measured, has to be at the same distance from the two horizontal lines that separate the segments [17]. $A_i$ values are calculeted by Eq. (6).

$$A_i = \int_{z_i}^{z_{i+1}} 2\sqrt{R^2 - (z - H)^2} dz \tag{6}$$

Where:

| | |
|---|---|
| $z_i$ | is the height of the $i$ th segment separation line |
| $R$ | is the rotor radius |
| $H$ | is the hub height |

On this study, two different wind turbines performance have been analyzed: DTU 10-MW Reference Wind Turbine with $178m$ of diameter [7] and NREL 5-MW with $126m$ of diameter [12]. Considering that the data set is composed with wind speed measurements each $20m$, the segments width have been fixed with the same distance. However, the top and bottom segments width is slightly smaller and hence the height which the wind velocity is measured is no located exactly on the segment middle. The segments distribution for both rotor areas are detailed on the tables (1) and (2). The weighting of each segment is calculated dividing its area by the rotor area.

| Measurement Heights [m] | Segment weighting [%] | Segment inferior limit height [m] | Segment superior limit height [m] | Segment height [m] |
|---|---|---|---|---|
| 200 | 5.73 | 190 | 209 | 19 |
| 180 | 10.49 | 170 | 190 | 20 |
| 160 | 12.74 | 150 | 170 | 20 |
| 140 | 13.91 | 130 | 150 | 20 |
| 120 | 14.28 | 110 | 130 | 20 |
| 100 | 13.91 | 90 | 110 | 20 |
| 80 | 12.74 | 70 | 90 | 20 |
| 60 | 10.49 | 50 | 70 | 20 |
| 40 | 5.73 | 31 | 50 | 19 |
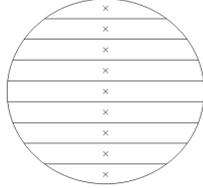
Table 1: Details of wind speed weighting for DTU 10-MW Wind Turbine. Hub height 120m

| Measurement Heights [m] | Segment weighting [%] | Segment inferior limit height [m] | Segment superior limit height [m] | Segment height [m] |
|---|---|---|---|---|
| 180 | 5.45 | 170 | 183 | 13 |
| 160 | 15.42 | 150 | 170 | 20 |
| 140 | 19.06 | 130 | 150 | 20 |
| 120 | 20.12 | 110 | 130 | 20 |
| 100 | 19.06 | 90 | 110 | 20 |
| 80 | 15.42 | 70 | 90 | 20 |
| 60 | 5.45 | 57 | 70 | 13 |
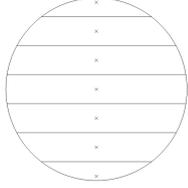
Table 2: Details of wind speed weighting for NREL 5-MW Wind Turbine. Hub height 120m

*2.4. Energy Estimation*

The generated power by the turbine due to wind speed is obtained through the wind turbine power curve. The power curves used in the study are interpolated from a Wind Speed - Power point list provided by the developers.

As it is showed on the tables (3) and (4), in both wind turbines the cut-in wind speed is 4 m/s, the rated wind speed is 12 m/s and the cut-out wind speed is 25 m/s.

| Wind Speed | Rotor Power |
|:---:|:---:|
| [m/s] | [kW] |
| 4 | 263,2 |
| 5 | 750,6 |
| 6 | 1.439,8 |
| 7 | 2.354,2 |
| 8 | 3.504,6 |
| 9 | 4.989,9 |
| 10 | 6.844,9 |
| 11 | 9.110,6 |
| 12-25 | 10.000 |
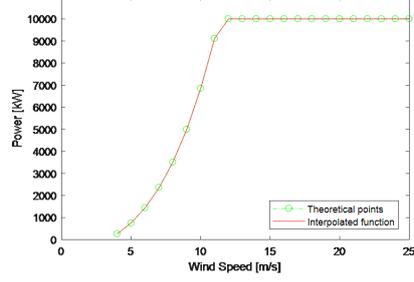


Table 3: DTU 10-MW Power Curve [3]

| Wind Speed | Rotor Power |
|:---:|:---:|
| [m/s] | [kW] |
| 4 | 177,7 |
| 5 | 403,9 |
| 6 | 737,3 |
| 7 | 1.187,2 |
| 8 | 1.771,1 |
| 9 | 2.518,6 |
| 10 | 3.448,4 |
| 11 | 4.562,5 |
| 12-25 | 5.000 |
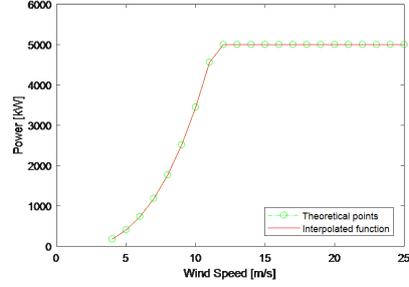


Table 4: NREL 5-MW Power Curve [1]

The Annual Energy Production is calculated by following IEC 61400-12-1 [5]. The power and the velocity are calculated using the bins method, with 0.5 m/s bins Eq. (7) and (8).

$$V_i = \frac{1}{N_i} \sum_{j=1}^{N_i} V_{n,i,j} \tag{7}$$

$$P_i = \frac{1}{N_i} \sum_{j=1}^{N_i} P_{n,i,j} \tag{8}$$

Finally, the AEP is estimated with the Eq. (9).

$$AEP = N_h \sum_{i=1}^{N} [F(V_i) - F(V_{i-1})] \left( \frac{P_{i-1} + P_i}{2} \right) \tag{9}$$

Where:

| | |
|---|---|
| $N_h$ | is the number of hours in one year (8760) |
| $N$ | is the number of bins |
| $V_i$ | is the averaged wind speed in bin $i$ |
| $P_i$ | is the averaged power output in bin $i$ |
| $F(V_i)$ | is the Rayleigh cumulative probability distribution for wind speed $V_i$ |

The power of each bin, calculated with Eq.(8), has to be applied to Rayleigh distribution. In this study, the wind distribution is known due the LIDAR measurements. Therefore, the AEP has been calculated for the Rayleigh distribution that best fits the LIDAR measured wind speed distribution. The measured wind speed distribution and the calculated Rayleigh distribution will be compared on chapter 4.

## 3. Wind Data Analysis

The study has been realised using the public wind data register from Hollandse Kust zuid (HKZ) wind farm zone location, in the Dutch sector of the North Sea, $23.5km$ far from the Dutch coast [2]. The site is composed of two Seawatch Lidar Buoys deployed by FUGRO OCEANOR, *HKZA* and *HKZB*, $2km$ separated from each other. For data availability reasons, only the data from *HKZB* has been used. The buoy, located at 52° 18′ N and 4° 32′ E, contains a waves and buoy motions sensor, two Vaisala sensors for aire pressure, humidity and temperature, and a ZephiR 300S LIDAR for wind speed. The LIDAR device measures wind speed and direction at 10 heights: 40, 60, 80, 100, 120, 140, 160, 180 and 200m. Hence, a Gill Windsonic M sensor, also installed in the buoy, measures the wind speed and direction at 4m.

(a)
(b)
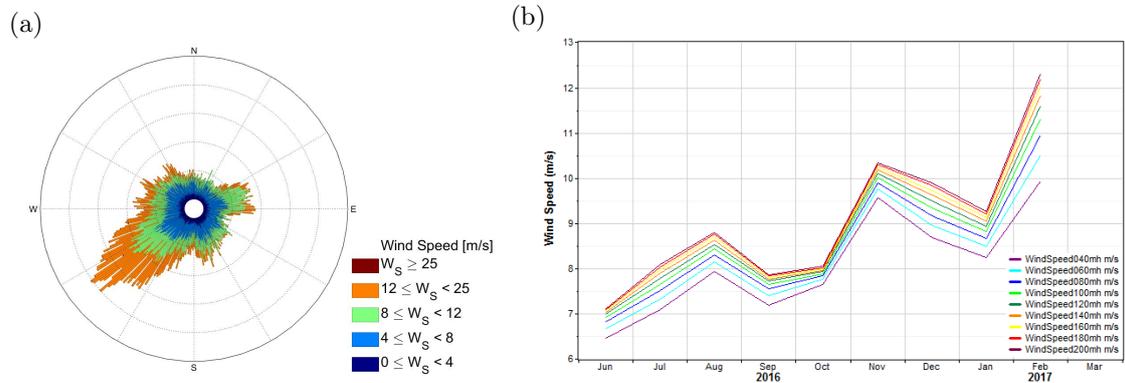


Figure 1: 120m wind speed wind rose (a). Monthly mean wind speed from 40 to 200m height (b).

The measurement campaign started on the $4^{th}$ of June 2016 at 10:20 GMT and still continues nowadays. However, the database used on the analysis is the data available on [2], from the starting date to March 2017. The whole data consists in 10-min averages which means a data set of 43.200 data points for each height. Unfortunely, the availability of the data in not complete due to different LIDAR technical issues and, therefore, the total number of data points after filtering is 41.931 (97.06%). As is shown on the Fig.(1a), the predominating wind direction is WSW, as usual at the north sea. The most part of the time, the wind speed is within the range [4-25] m/s. As showed on chapter (2), that means a wind turbine would be most part of the time producing energy under these conditions. As may be seen on the figure (1b), the monthly mean wind speed increases with the height. In all the months, the wind speed at certain height is higher

than the wind speed at a lower height. The monthly wind speed difference vary each month, from $\approx 0.5$m/s in October to $\approx 2.5$m/s in February and it can be appreciated that the mean wind speeds at summer months (from June to September) are clearly lower than the wind velocities at winter months.

For the better understanding of these results and the final results on the next chapter, is necessary to describe the assumptions and simplifications done for the analysis. The study of floating LIDAR uncertainties is an important subject matter nowadays. Wolken-Möhlmann and Lange [18] establish four measurement errors because of the system motion and prove with their results that the influence of the movement can not be negligible. These errors are due to the interference of the system motion, the system tilt angle that modifies the beam projection, the system height that change the measure point height and finally, the combination of the previous three. In other study, Gottschall [10] specifies the system motion and the waves height does not affect the horizontal wind speed measurement. In her results, the LIDAR measurements had a very good agreement with the met mast results (Coefficient of determination = 0.996). On the other hand, the results for the wind direction and turbulence showed the system motion influence on them and the need to a motion correction algorithm.

As said on the beginning of this chapter, it only has been used the public database which does not include the buoy motion data such as roll and pitch. Therefore, a correction algorithm has not been implemented to the data. The only information related to the data reliability are the monthly validation reports available on [2]. On the reports, the scatter wind speed and direction plots show a good agreement between the measurements at HKZA and HKZB buoys Fig. (2).
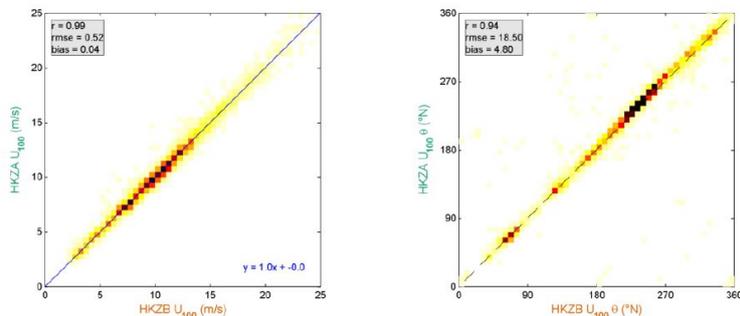


Figure 2: Direct scatter comparison sample between buoy wind at elevations of 100 and 160m corresponding to March 2017 period. [2]

## 4. Results

The average ABL of the whole database, showed on Fig.(3), has a characteristic exponential shape. The MBL interpolation results for the LL and PL are excellent with MSE equal to 0.0031 and 0.093 respectively. Although, the STD wind shear coefficient (0.14) does not correspond to the calculated and the MSE is 0.3270.
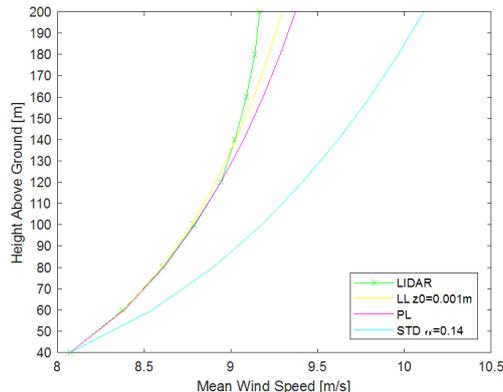
Figure 3: Interpolation results for the MBL

However, the results for the interpolation on each 10-min data differ of the previous. The Mean MSE (Table 5, column 6) are higher for all ABL estimation methods. The PL reaches the best results with a $MSE = 0.2435$. For the LL the MSE outweight the unit, instead. The maximum MSE values obtained in all methods are obtained in those time points where the wind speed component at 40m is very small comparing with the wind speed at hub height. That situation is produced when there is a big variation on the wind direction of both heights. For the PL method, the calculated wind shear coefficient is very high resulting an overestimated wind speed at high heights. Exactly the opposite occurs for the LL estimation, due to the small z0, the boundary layer is almost vertical. When the wind speed difference is big, there is an underestimation of the wind velocity at high heights again.

| Method | Shear coefficient | MSE of MBL | Max. MSE from 10-min data | Min. MSE from 10-min data | Mean MSE from 10-min data |
|--------|--------|--------|--------|--------|--------|
| LL | - | 0.0031 | 19.9543 | $\approx 0$ | 1.1016 |
| PL | 0.093 | 0.0087 | 19.4593 | $\approx 0$ | 0.2435 |
| STD | 0.140 | 0.3270 | 19.8849 | $\approx 0$ | 1.4920 |

Table 5: Interpolation errors from each interpolation method

The results reveal the exponential shape assumption that, PL and LL make for the ABL, is only valid for a long time periods and the BL shape has not an exponential function shape at all time points.

The measured mean wind speed an 120m height (Hub Height), Table (6), is 8.94 m/s. Only the STD method presents a poor result with an increment of 5.3%, while, the mean HH wind speed for LL is 0.3% lower (coinciding with Fig.(3). Other important aspect to emphasize is the difference between the hub height velocity and the REWS. In all cases the REWS is lower than the HH wind speed, obtaining the highest difference for the LIDAR measurements, −0.78%, followed by LL with −0.63% m/s, the STD with −0.57% and finally the PL method with −0.21%.

|  | Mean HH wind speed [m/s] |  | Difference between REWS and HH wind speed [m/s] |
|---|---|---|---|
| LIDAR | 8.94 | LIDAR | -0.070 |
| LL | 8.91 | LL | -0.051 |
| PL | 8.94 | PL | -0.018 |
| STD | 9.41 | STD | -0.060 |

Table 6: Hub Height wind speed and REWS comparison for DTU 10-MW

The monthly power production comparison for the DTU 10-MW and NREL 5-MW are presented on the figure(4). The figure (a) shows the results for all methods when the hub height wind speed is used whilst the figure (b) shows the power production when the REWs is used. As expected, in all cases the power production for LIDAR measurements and PL using HH wind speed is exactly the same and, the variation when the REWS is used is very small.

The power production using LL is higher than the LIDAR's in spite of the lower mean wind speed at hub height. That could be caused by a combination of several causes. The hub height underestimation for LL when the wind speed at 40m is very small ,explained in chapter (2), contribute to decrease the average HH wind speed. However, for hub height wind speeds higher than 12 m/s, the power production is constant. Considering that the absolute mean wind velocity difference between 40 and 120m is 0.83% for LL and 0.95% for LIDAR, it is possible producing the same amount of energy with lower wind speed. The last aspect for consideration is that the ABL measured with LIDAR contains many time points where the wind speed at hub height is lower than the wind speed at the bottom, that never happens for the LL boundary layer due to the logarithmic function shape. In that case, the HH overestimation of LL, could be counterbalanced by the previous cases but, in this case, the power production would be higher for the LL.

The STD has the biggest power production in all cases. It can be noted on the figure (c) that the power production difference in using HH wind speed or REWS is near 0, according to the mean wind speed difference on Table (6). The Fig. (4) also reveals the Power production and rotor size linearity relation. In all cases the estimated power for the DTU 10-MW is around $98 - 99\%$ higher than the produced by the NREL 5-MW.

(a)



(b)



(c)
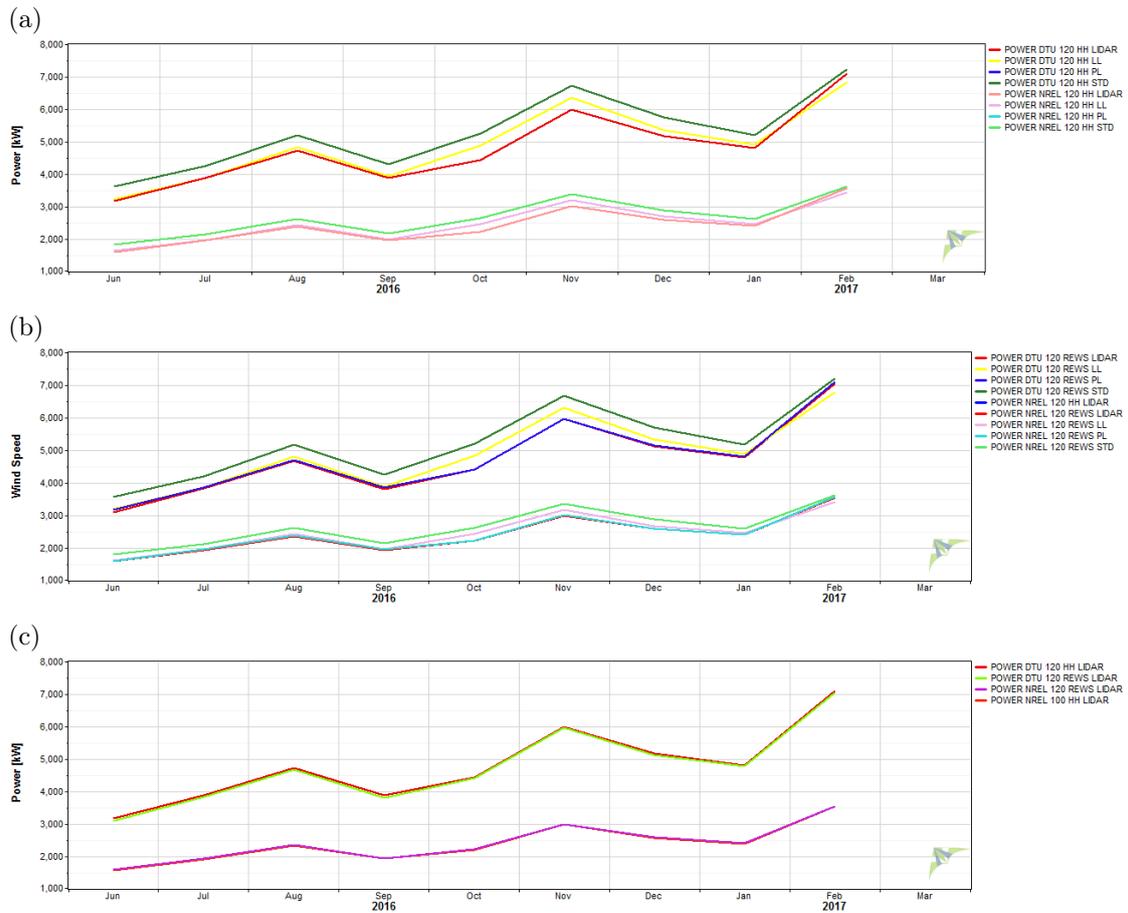


Figure 4: Power production from DTU 10-MW (Hub height at 120m) for (a) Hub Height wind speed and (b) REWS. (c) Comparison between LIDAR Hub Height wind speed and REWS

As is said on chapter (2), according to IEC 61400-12-1 [5] the AEP has to be calculated using the Rayleigh cumulative probability distribution[1]. On the Fig.(5), the wind distribution fits with a great degree of success the Rayleigh distribution, anyway the AEP for both probability distribution has been calculated.

(a)

(b)
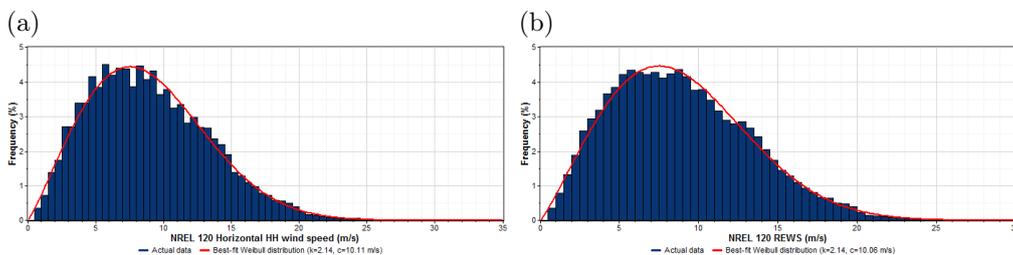


Figure 5: Wind speed histogram and Rayleigh distribution for NREL 10-MW (HH at 120m) (a) REWS and (b) Lidar HH wind speed

The AEP for the NREL 5-MW are shown in the table (7). For the LIDAR measurements and the PL method, the obtained results when using the histogram

---

[1] The Weibull distribution with the "shape parameter" k=2 yields a Rayleigh distribution.

probability are around $\approx 1.3\%$ lower, for the LL the results are $\approx 0.5\%$ higher and finally for STD the AEP is $\approx (1.25 - 1.35)\%$ higher. The comparison between HH and REWS energy production is more clear. For all the methods, regardless the probability used, the AEP using HH wind speed is slightly higher. The difference varies for each method being: $\approx 0.2\%$ for PL, $\approx 0.4\%$ for LL and STD, and $\approx 0.6\%$ for LIDAR measurements.

|  | LIDAR | LL | PL | STD |
|---|---|---|---|---|
| REWS (RAYLEIGH) | 21.07 | 20.87 | 21.15 | 22.34 |
| REWS (HISTOGRAM) | 20.79 | 20.97 | 20.88 | 22.61 |
| HH (RAYLEIGH) | 21.20 | 20.95 | 21.20 | 22.42 |
| HH (HISTOGRAM) | 20.91 | 21.06 | 20.91 | 22.70 |

Table 7: AEP (MWh) for NREL 5-MW (Hub Height at 120m)

Finally comparing the performance of three methods, the STD method overestimate the energy production $\approx (5.5 - 8.5)\%$ depending the probability used. The PL has the most accurate results, $\approx +0.4\%$ using REWS and the same result using HH wind speed. The LL results are $\approx (0.7 - 0.9)\%$ higher when the histogram probability is used and $\approx (1-1.2)\%$ lower when the Rayleigh probability is used. The results for the NREL when the HH is at 100m are $\approx (1.5 - 3)\%$ lower depending the method and the probability distribution used.

## 5. Conclusion

Three common atmospheric prediction methods have been analysed against floating buoy LIDAR measurements and an AEP for DTU-10MW and NREL 5-MW have been estimated. On the one hand, the results reveal the excelent performance of LL and PL for estimating the mean boundary layer for a long time period. On the other hand, none of three have reliable results when only one time point is predicted.It is important to mention that the buoy motion has not been considered for LIDAR measurements which is an uncertainly cause and it could be interesting to study its real effect on them.

The purpose of the REWS is to establish a representative wind speed over the wind turbine rotor for reaching a more accurate energy estimation. The results show the REWS is slightly below the HH wind speed for all studied methods. The maximum difference is 0.07 m/s for the LIDAR measurements and consequently the AEP is 0.6% lower. In power results, that means the underestimation of AEP using REWS is only around $0.2 - 0.4\%$ than the AEP using HH wind speed. Regarding to the turbines results, the power difference between the NREL 5-MW with hub height at 100 or at 120m is $\approx (1.5 - 3)\%$ depending the method used.

**References**
 [1] NREL 5-MW reference turbine - NWTC.
 [2] Offshorewind.rvo.nl.
 [3] The DTU 10MW Reference Wind Turbine Project Site.
 [4] The Future of Wind Power | Planète Énergies.

[5] International standard IEC 61400-12-1 Ed.1: Power performance measurements of electricity producing wind turbines. page 76, 2005.

[6] REWS EWEA Power Curve Working Group. 2014.

[7] C. Bak, F. Zahle, R. Bitsche, and T. Kim. The DTU 10-MW reference wind turbine. *Danish wind power*, 2013.

[8] International Electrotechical Commision. IEC 61400-3. Wind Turbines-Part 3: Design Requierments for Offshore Wind Turbines. 2009.

[9] S. Fechner and L. Saetran. Preprosessering av meteorologiske data for atmosfaeriske teoretisk/numeriske modeller Preprocessing of meteorological data for atmospheric theoretical/numerical models. 2015.

[10] J. Gottschall, G. Wolken-Möhlmanna, T. Viergutza, and B. Langea. Results and conclusions of a floating-lidar offshore test. 2014.

[11] A. Honrubia, A. Vigueras-Rodríguez, E. Gómez Lázaro, and D. Rodíguez-Sánchez. The influence of wind shear in wind turbine power estimation. *Proceeding of EWEA2009, Stockholm (2009)*, 2009.

[12] J. Jonkman, S. Butterfield, W. Musial, and G. Scott. Definition of a 5-MW reference wind turbine for offshore system development. *Contract*, (February):1–75, 2009.

[13] F. Lizák and P. Semančík. Intensive Programme "Environmental Impacts of Power Industry" Evolution and Future of Wind Energy in Europe.

[14] Det Norske Veritas. Environmental conditions and environmental loads. 2010.

[15] Günther H Oettinger. Energy roadmap 2050.

[16] A. Peña, C. B. Hasager, M. Badger, R. J. Barthelmie, F. Bingöl, J. Cariou, S. Emeis, S. T. Frandsen, M. Harris, I. Karagali, S. E. Larsen, J. Mann, T. Mikkelsen, M. Pitter, S. Pryor, A. Sathe, D. Schlipf, C. Slinger, and R. Wagner. *Remote Sensing for Wind Energy DTU Wind Energy E-Report Remote Sensing for Wind Energy*, volume E-Report-0. 2015.

[17] R Wagner, B Cañadillas, A Clifton, S Feeney, N Nygaard, M Poodt, C St Martin, E Tüxen, and J W Wagenaar. Rotor equivalent wind speed for power curve measurement – comparative exercise for IEA Wind Annex 32. *Journal of Physics: Conference Series*, 524:012108, 2014.

[18] G. Wolken-Möhlmann, H. Lilov, and B. Lange. Simulation of motion induced measurement errors for wind measurements using LIDAR on floating platforms.